

All-Microwave Leakage Reduction Units for Quantum Error Correction with Superconducting Transmon Qubits

J. F. Marques^{1,2}, H. Ali^{1,2}, B. M. Varbanov¹, M. Finkel^{1,2}, H. M. Veen^{1,2}, S. L. M. van der Meer^{1,2}, S. Valles-Sanclemente^{1,2}, N. Muthusubramanian^{1,2}, M. Beekman^{1,3}, N. Haider^{1,3}, B. M. Terhal^{1,4} and L. DiCarlo^{1,2,*}

¹*QuTech, Delft University of Technology, P.O. Box 5046, 2600 GA Delft, Netherlands*

²*Kavli Institute of Nanoscience, Delft University of Technology, P.O. Box 5046, 2600 GA Delft, Netherlands*

³*Netherlands Organisation for Applied Scientific Research (TNO), P.O. Box 96864, 2509 JG The Hague, Netherlands*

⁴*EEMCS Department, Delft University of Technology, P.O. Box 5046, 2600 GA Delft, Netherlands*



(Received 22 March 2023; accepted 24 May 2023; published 22 June 2023)

Minimizing leakage from computational states is a challenge when using many-level systems like superconducting quantum circuits as qubits. We realize and extend the quantum-hardware-efficient, all-microwave leakage reduction unit (LRU) for transmons in a circuit QED architecture proposed by Battistel *et al.* This LRU effectively reduces leakage in the second- and third-excited transmon states with up to 99% efficacy in 220 ns, with minimum impact on the qubit subspace. As a first application in the context of quantum error correction, we show how multiple simultaneous LRUs can reduce the error detection rate and suppress leakage buildup within 1% in data and ancilla qubits over 50 cycles of a weight-2 stabilizer measurement.

DOI: [10.1103/PhysRevLett.130.250602](https://doi.org/10.1103/PhysRevLett.130.250602)

Introduction.—Superconducting qubits, such as the transmon [1], are many-level systems in which a qubit is represented by the two lowest-energy states $|g\rangle$ and $|e\rangle$. However, leakage to noncomputational states is a risk for all quantum operations, including single-qubit gates [2], two-qubit gates [3–5], and measurement [6,7]. While the typical probability of leakage per operation may pale in comparison to conventional qubit errors induced by control errors and decoherence [5,8], unmitigated leakage can build up with increasing circuit depth. A prominent example is multiround quantum error correction (QEC) with stabilizer codes such as the surface code [9]. In the absence of leakage, such codes successfully discretize all qubit errors into Pauli errors through the measurement of stabilizer operators [10,11], and these Pauli errors can be detected and corrected (or kept track of) using a decoder. However, leakage errors fall outside the qubit subspace and are not immediately correctable [12–14]. The signature of leakage on the stabilizer syndrome is often not straightforward, hampering the ability to detect and correct it [15,16]. Additionally, the buildup of leakage over QEC rounds accelerates the destruction of the logical information [8,17]. Therefore, despite having low probability per operation, methods to reduce leakage must be employed when performing experimental QEC with multilevel systems.

Physical implementations of QEC codes [18–23] use qubits for two distinct functions: data qubits store the logical information and, together, comprise the encoded logical qubits. Ancilla qubits perform indirect measurement of the stabilizer operators. Handling leakage in ancilla qubits is relatively straightforward as they are measured in

every QEC cycle. This allows for the use of reset protocols [17,24] without the loss of logical information. Leakage events can also be directly detected using three- or higher-level readout [19] and reset using feedback [25,26]. In contrast, handling data-qubit leakage requires a subtle approach as it cannot be reset nor directly measured without loss of information or added circuit complexity [27–29]. A promising solution is to interleave QEC cycles with operations that induce seepage without disturbing the qubit subspace, known as leakage reduction units (LRUs) [12,13,27,28,30–34]. An ideal LRU returns leakage back to the qubit subspace, converting it into Pauli errors which can be detected and corrected, while leaving qubit states undisturbed. By converting leakage into conventional errors, LRUs enable a moderately high physical noise threshold, below which the logical error rate decreases exponentially with the code distance [13,28]. A more powerful operation called “heralded leakage reduction” would both reduce and herald leakage, leading to a so-called erasure error [35,36]. Unlike Pauli errors, the exact location of erasures is known, making them easier to correct and leading to higher error thresholds [37–40].

In this Letter, we present the realization and extension of the LRU scheme proposed in Ref. [33]. This is a highly practical scheme requiring only microwave pulses and the quantum hardware typically found in contemporary circuit QED quantum processors: a microwave drive and a readout resonator dispersively coupled to the target transmon (in our case, a readout resonator with a dedicated Purcell filter). We show its straightforward calibration and the effective removal of the population in the first two leakage

states of the transmon ($|f\rangle$ and $|h\rangle$) with up to $> 99\%$ efficacy in 220 ns. Process tomography reveals that the LRU backaction on the qubit subspace is only an ac-Stark shift, which can be easily corrected using a Z-axis rotation. As a first application in a QEC setting, we interleave repeated measurements of a weight-2 parity check [16,26] with simultaneous LRUs on data and ancilla qubits, showing the suppression of leakage and error detection rate buildup.

Results.—Our leakage reduction scheme [Fig. 1(a)] consists of a transmon with states $|g\rangle$, $|e\rangle$, and $|f\rangle$, driven by an external drive Ω , coupled to a resonant pair of Purcell and readout resonators [41] with effective dressed states $|00\rangle$ and $|1^\pm\rangle$. The LRU scheme transfers leakage population in the second-excited state of the transmon, $|f\rangle$, to the ground state, $|g\rangle$, via the resonators using a microwave drive. It does so using an effective coupling, \tilde{g} , mediated by the transmon-resonator coupling, g , and the drive Ω , which

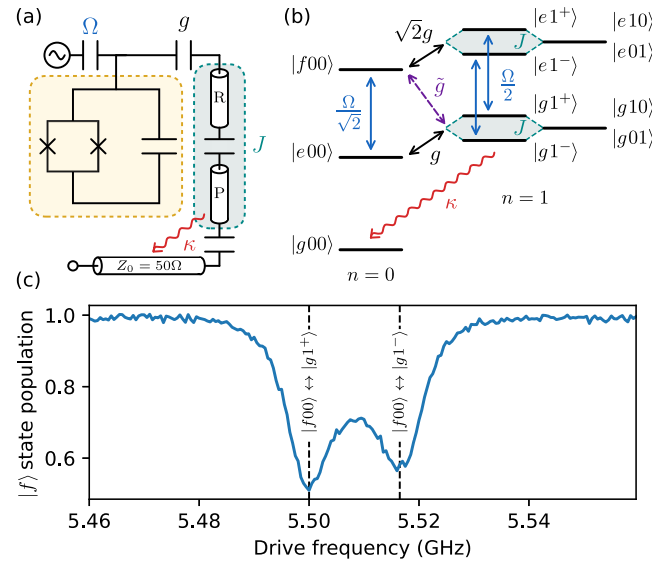


FIG. 1. Leakage reduction unit scheme. (a) Schematic for the driven transmon-resonator system. A transmon (T , yellow) with three lowest-energy levels $|g\rangle$, $|e\rangle$, and $|f\rangle$ is coupled to a readout resonator (R) with strength g . The latter is coupled to a frequency-matched Purcell resonator (P) with strength J . The Purcell resonator also couples to a $50\ \Omega$ feedline through which its excitations quickly decay at rate κ . The transmon is driven with a pulse of strength Ω applied to its microwave drive line. (b) Energy level spectrum of the system. Levels are denoted as $|T, R, P\rangle$, with numbers indicating photons in R and P . As the two resonators are frequency matched, the right-most degenerate states split by $2J$, and g is shared equally among the two hybridized resonator modes $|1^- \rangle$ and $|1^+ \rangle$. An effective coupling \tilde{g} arises between $|f00\rangle$ and the two hybridized states $|g1^\pm\rangle$ via $|e00\rangle$ and $|e1^\pm\rangle$. (c) Spectroscopy of the $|f00\rangle \leftrightarrow |g1^\pm\rangle$ transition. Measured transmon population in $|f\rangle$ versus drive frequency, showing dips corresponding to the two transitions assisted by each of the hybridized resonator modes.

couple states $|f00\rangle$ and $|g1^\pm\rangle$. Driving at the frequency of this transition,

$$\omega_{f00} - \omega_{g1^\pm} \approx 2\omega_Q + \alpha - \omega_{RP}, \quad (1)$$

transfers population from $|f00\rangle$ to $|g1^\pm\rangle$, which in turn quickly decays to $|g00\rangle$ provided the transition rate, \tilde{g} , is small compared to κ . Here, ω_Q and α are the transmon qubit transition frequency and anharmonicity, respectively, while ω_{RP} is the resonator mode frequency. In this regime, the drive effectively pumps any leakage in $|f\rangle$ to the computational state $|g\rangle$. We perform spectroscopy of this transition by initializing the transmon in $|f\rangle$ and sweeping the drive around the expected frequency. The results [Fig. 1(c)] show two dips in the f -state population corresponding to transitions with the hybridized modes of the matched readout-Purcell resonator pair. The dips are broadened by $\sim \kappa_{\text{eff}}/2\pi \approx 8$ MHz, where $\kappa_{\text{eff}} = \kappa/2$ is the effective linewidth of the dressed resonator (see Ref. [42] for device characteristics and metrics), making them easy to find. We achieve typical couplings of $\tilde{g}/2\pi \sim 1$ MHz for this transition [42].

To make use of this scheme for a LRU, we calibrate a pulse that can be used as a circuit-level operation. We use the pulse envelope proposed in Ref. [33]:

$$A(t) = \begin{cases} A \sin^2\left(\pi \frac{t}{2t_r}\right) & \text{for } 0 \leq t \leq t_r, \\ A & \text{for } t_r \leq t \leq t_p - t_r, \\ A \sin^2\left(\pi \frac{t_p - t}{2t_r}\right) & \text{for } t_p - t_r \leq t \leq t_p, \end{cases} \quad (2)$$

where A is the amplitude, t_r is the rise and fall time, and t_p is the total duration. We conservatively choose $t_r = 30$ ns to avoid unwanted transitions in the transmon. To measure the fraction of leakage removed, R , we apply the pulse on the transmon prepared in $|f\rangle$ and measure it [Fig. 2(a)], correcting for readout error using the measured 3-level assignment fidelity matrix [Fig. 2(c)]. To optimize the pulse parameters, we first measure R while sweeping the pulse frequency and A [Fig. 2(d)]. A second sweep of t_p and A [Fig. 2(e)] shows that $R > 99\%$ can be achieved by increasing either parameters. This value is limited by thermal population in the resonator modes. We estimate values of $P(n=1) \approx 0.5\%$ [42]. Simulation [33] suggests that $R \approx 80\%$ is already sufficient to suppress most of the impact of current leakage rates, which is comfortably achieved over a large region of parameter space. For QEC, a fast operation is desirable to minimize the impact of decoherence. However, one must not excessively drive the transmon, which can cause extra decoherence (see Fig. 6 in Ref. [33]). Considering the factors above, we opt for $t_p = 220$ ns and adjust A such that $R \gtrsim 80\%$. Additionally, we benchmark the repeated action of the LRU and verify that its performance is maintained over

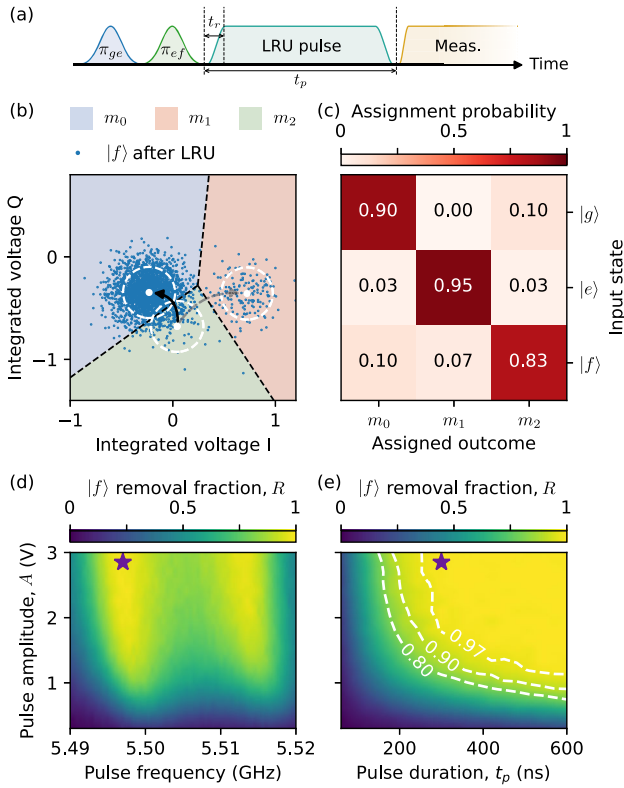


FIG. 2. Calibration of the leakage reduction unit pulse. (a) Pulse sequence used for LRU calibration. (b) Single-shot readout data obtained from the experiment. The blue, red, and green areas denote m_0 , m_1 , and m_2 assignment regions, respectively. The mean (white dots) and 3σ standard deviation (white dashed circles) shown are obtained from Gaussian fits to the three input-state distributions. The blue data show the first 3×10^3 (from a total of 2^{15}) shots of the experiment described in (a), indicating 99.(3)% $|f\rangle$ -state removal fraction. (c) Measured assignment fidelity matrix used for readout correction. (d),(e) Extracted $|f\rangle$ -state removal fraction versus pulse parameters. Added contours (white dashed curves) indicate 80%, 90%, and 97% removal fraction. The purple star indicates the pulse parameters used in (b).

repeated applications, thus restricting leakage events to approximately a single cycle (see Fig. S2 [42]).

With the LRU calibrated, we then benchmark its impact on the qubit subspace using quantum process tomography. The results (Fig. 3) show that the qubit incurs a Z-axis rotation. We find that the rotation angle increases linearly with t_p [Fig. 3(g)], consistent with a 71(9) kHz ac-Stark shift induced by the LRU drive. This phase error in the qubit subspace can be avoided using decoupling pulses or corrected with a virtual Z gate. Figures 3(h) and 3(i) show the Pauli transfer matrix (PTM) for the operation before and after applying a virtual Z correction, respectively. From the measured PTM [Fig. 3(i)] and enforcing physicality constraints [43], we obtain an average gate fidelity $F_{\text{avg}} = 98.(9)\%$. Compared to the measured 99.(2)% fidelity of idling during the same time ($t_p = 220$ ns), there is evidently no significant error increase.

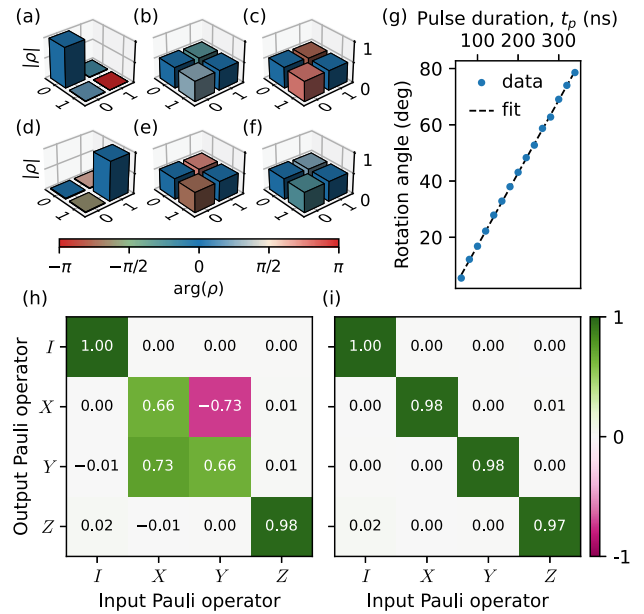


FIG. 3. Process tomography of the leakage reduction unit. (a)–(f) Measured density matrices after the LRU gate for input states $|0\rangle$, $|+\rangle$, $|+i\rangle$, $|1\rangle$, $|-\rangle$, and $|-i\rangle$, respectively. (g) Z-rotation angle induced on the qubit versus the LRU pulse duration. The linear best fit (black dashed line) indicates an ac-Stark shift of 71(9) kHz. (h),(i) Pauli transfer matrix of the LRU with (i) and without (h) virtual phase correction [$t_p = 220$ ns and $R = 84.(7)\%$].

Finally, we implement the LRU in a QEC scenario by performing repeated stabilizer measurements of a weight-2X-type parity check [16,26] using three transmons (Fig. 4). We use the transmon in Figs. 1–3, D_1 , plus an additional transmon (D_2) as data qubits together with an ancilla, A . LRUs for D_2 and A are tuned using the same procedure as above. A detailed study of the performance of this parity check and of the impact of simultaneous LRUs is shown in [42] Figs. S6 and S5. Given their frequency configuration [44], D_1 and A are most vulnerable to leakage during two-qubit controlled-Z (CZ) gates, as shown by the avoided crossings in Fig. 4(a). Additional leakage can occur during other operations: in particular, we observe that leakage into states above $|f\rangle$ can occur in A due to measurement-induced transitions [6] (see Fig. S10 [42]). Therefore, a LRU acting on $|f\rangle$ alone is insufficient for A . To address this, we develop an additional LRU for $|h\rangle$ (h -LRU), the third-excited state of A (see Fig. S9 [42]). The h -LRU can be employed simultaneously with the f -LRU without additional cost in time or impact on the $|f\rangle$ removal fraction, R . Thus, we simultaneously employ f -LRUs for all three qubits and an h -LRU for A [Fig. 4(a)]. To evaluate the impact of the LRUs, we measure the error detection probability (probability of a flip occurring in the measured stabilizer parity) and leakage population of the three transmons over multiple rounds of stabilizer measurement. Without leakage reduction, the error detection probability

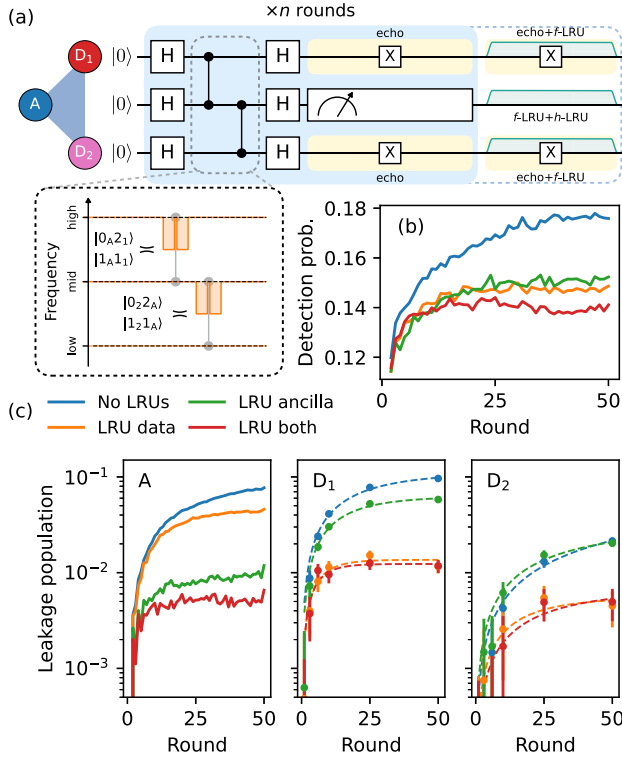


FIG. 4. Repeated stabilizer measurement with leakage reduction. (a) Quantum circuit using ancilla A to measure the X -type parity of data qubits D_1 and D_2 . The dashed box shows the frequency arrangement for two-qubit CZ gates. A CZ gate is performed by fluxing the higher-frequency transmon down in frequency to the nearest avoided crossing (orange shaded trajectory). The duration of single-qubit gates, CZ gates, and measurement are 20, 60, and 340 ns, respectively, totalling 500 ns for the parity check (light-blue region). Performing the LRUs extends the circuit by 220 ns (blue-dashed region). Echo pulses on data qubits mitigate phase errors caused by residual ZZ crosstalk and ac-Stark shift during the measurement and LRUs (light yellow slots). (b),(c) Measured error-detection probability (b) and leakage (c) versus the number of parity-check rounds in four settings. Here, leakage includes any population outside the computational subspace. The “No LRUs” setting (blue) does not apply any LRUs. LRU data (orange) and LRU ancilla (green) settings apply LRUs exclusively on the data qubits and the ancilla, respectively. The LRU both (red) setting applies LRUs on all qubits.

rises $\sim 8\%$ in 50 rounds. We attribute this feature to leakage buildup [17,22,34]. With the LRUs, the rise stabilizes faster (in ~ 10 rounds) to a lower value and is limited to 2%, despite the longer cycle duration (500 versus 720 ns without and with the LRU, respectively). Leakage is overall higher without LRUs, in particular for D_1 and A [Fig. 4(c)], which show a steady-state population of $\approx 10\%$. Using leakage reduction, we lower the leakage steady-state population by up to one order of magnitude to $\lesssim 1\%$ for all transmons. Additionally, we find that removing leakage on other transmons leads to lower overall leakage,

suggesting that leakage is transferred between transmons [15,34]. This is particularly noticeable in A [Fig. 4(c)], where the steady-state leakage is always reduced by adding LRUs on D_1 and D_2 .

Discussion.—We have demonstrated and extended the all-microwave LRU for superconducting qubits in circuit QED proposed in Ref. [33]. We have shown how these LRUs can be calibrated using a straightforward procedure to deplete leakage in the second- and third-excited states of the transmon. This scheme could potentially work for even higher transmon states using additional drives. We have verified that the LRU operation has minimal impact in the qubit subspace, provided one can correct for the static ac-Stark shift induced by the drive(s).

This scheme does not reset the qubit state and is therefore compatible with both data and ancilla qubits in the QEC context. We have showcased the benefit of the LRU in a building-block QEC experiment where LRUs decrease the steady-state leakage population of data and ancilla qubits by up to one order of magnitude (to $\lesssim 1\%$), and thereby reduce the error detection probability of the stabilizer and reaching a faster steady state. We find that the remaining ancilla leakage is dominated by higher states above $|f\rangle$ (see Fig. S10 [42]) likely caused by the readout [6,7]. Given the observation leakage transfer between transmons, which can result in higher excited leakage states [34], data qubits can also potentially benefit from h -LRUs. Compared to other LRU approaches [17,34], we believe this scheme is especially practical as it is all-microwave and very quantum-hardware efficient, requiring only the microwave drive line and dispersively coupled resonator that are already commonly found in the majority of circuit QED quantum processors [19,20,22]. Extending this leakage reduction method to larger QEC experiments can be done without further penalty in time as all LRUs can be simultaneously applied. However, we note that when extending the LRU to many qubits, microwave crosstalk should be taken into account in order to avoid driving unwanted transitions. This can be easily avoided by choosing an appropriate resonator-qubit detuning.

The data supporting the plots and claims within this Letter are available online at [49]. Further data can be provided upon reasonable request.

We thank F. Battistel and Y. Herasymenko for helpful discussions, and G. Calusine and W. Oliver for providing the traveling-wave parametric amplifiers used in the readout amplification chain. This research is supported by the Office of the Director of National Intelligence (ODNI), Intelligence Advanced Research Projects Activity (IARPA), via the U.S. Army Research Office Grant No. W911NF-16-1-0071, by Intel Corporation, and by QuTech NWO funding 2021-2026—Part I “Fundamental Research,” Project No. 601.QT.001-1, financed by the Dutch Research Council (NWO). The views and

conclusions contained herein are those of the authors and should not be interpreted as necessarily representing the official policies or endorsements, either expressed or implied, of the ODNI, IARPA, or the U.S. Government.

J. F. M and H. A. contributed equally to this work. The authors declare no competing interests.

*Corresponding author.

l.dicarlo@tudelft.nl

- [1] J. Koch, T. M. Yu, J. Gambetta, A. A. Houck, D. I. Schuster, J. Majer, A. Blais, M. H. Devoret, S. M. Girvin, and R. J. Schoelkopf, Charge-insensitive qubit design derived from the Cooper pair box, *Phys. Rev. A* **76**, 042319 (2007).
- [2] F. Motzoi, J. M. Gambetta, P. Rebentrost, and F. K. Wilhelm, Simple Pulses for Elimination of Leakage in Weakly Nonlinear Qubits, *Phys. Rev. Lett.* **103**, 110501 (2009).
- [3] L. DiCarlo *et al.*, Demonstration of two-qubit algorithms with a superconducting quantum processor, *Nature (London)* **460**, 240 (2009).
- [4] R. Barends, C. M. Quintana, A. G. Petukhov, Y. Chen, D. Kafri *et al.*, Diabatic Gates for Frequency-Tunable Superconducting Qubits, *Phys. Rev. Lett.* **123**, 210501 (2019).
- [5] V. Negîrneac *et al.*, High-Fidelity Controlled- z Gate with Maximal Intermediate Leakage Operating at the Speed Limit in a Superconducting Quantum Processor, *Phys. Rev. Lett.* **126**, 220502 (2021).
- [6] D. Sank, Z. Chen, M. Khezri, J. Kelly, R. Barends *et al.*, Measurement-Induced State Transitions in a Superconducting Qubit: Beyond the Rotating Wave Approximation, *Phys. Rev. Lett.* **117**, 190503 (2016).
- [7] M. Khezri *et al.*, Measurement-induced state transitions in a superconducting qubit: Within the rotating wave approximation, [arXiv:2212.05097](https://arxiv.org/abs/2212.05097).
- [8] Z. Chen *et al.*, Exponential suppression of bit or phase errors with cyclic error correction, *Nature (London)* **595**, 383 (2021).
- [9] A. G. Fowler, M. Mariantoni, J. M. Martinis, and A. N. Cleland, Surface codes: Towards practical large-scale quantum computation, *Phys. Rev. A* **86**, 032324 (2012).
- [10] D. Ristè, S. Poletto, M.-Z. Huang, A. Bruno, V. Vesterinen, O.-P. Saira, and L. DiCarlo, Detecting bit-flip errors in a logical qubit using stabilizer measurements, *Nat. Commun.* **6**, 6983 (2015).
- [11] M. Takita, A. W. Cross, A. D. Córcoles, J. M. Chow, and J. M. Gambetta, Experimental Demonstration of Fault-Tolerant State Preparation with Superconducting Qubits, *Phys. Rev. Lett.* **119**, 180501 (2017).
- [12] P. Aliferis and B. M. Terhal, Fault-tolerant quantum computation for local leakage faults, *Quantum Inf. Comput.* **7**, 139 (2007).
- [13] A. G. Fowler, Coping with qubit leakage in topological codes, *Phys. Rev. A* **88**, 042308 (2013).
- [14] J. Ghosh, A. G. Fowler, J. M. Martinis, and M. R. Geller, Understanding the effects of leakage in superconducting quantum-error-detection circuits, *Phys. Rev. A* **88**, 062329 (2013).
- [15] B. M. Varbanov, F. Battistel, B. M. Tarasinski, V. P. Ostroukh, T. E. O'Brien, L. DiCarlo, and B. M. Terhal, Leakage detection for a transmon-based surface code, *npj Quantum Inf.* **6**, 102 (2020).
- [16] C. C. Bultink *et al.*, Protecting quantum entanglement from leakage and qubit errors via repetitive parity measurements, *Sci. Adv.* **6**, eaay3050 (2020).
- [17] M. McEwen, S. E. L. Howell, M. Brady, X. Xu, and K. McNeil, Removing leakage-induced correlated errors in superconducting quantum error correction, *Nat. Commun.* **12**, 1 (2021).
- [18] C. Ryan-Anderson, J. G. Bohnet, K. Lee, D. Gresh, A. Hankin *et al.*, Realization of Real-Time Fault-Tolerant Quantum Error Correction, *Phys. Rev. X* **11**, 041058 (2021).
- [19] S. Krinner *et al.*, Realizing repeated quantum error correction in a distance-three surface code, *Nature (London)* **605**, 669 (2022).
- [20] Y. Zhao, Y. Ye, H. L. Huang, Y. Zhang, D. Wu *et al.*, Realization of an Error-Correcting Surface Code with Superconducting Qubits, *Phys. Rev. Lett.* **129**, 030501 (2022).
- [21] N. Sundaresan *et al.*, Matching and maximum likelihood decoding of a multi-round subsystem quantum error correction experiment, [arXiv:2203.07205](https://arxiv.org/abs/2203.07205).
- [22] R. Acharya *et al.*, Suppressing quantum errors by scaling a surface code logical qubit, [arXiv:2207.06431](https://arxiv.org/abs/2207.06431).
- [23] L. Postler *et al.*, Demonstration of fault-tolerant universal quantum gate operations, *Nature (London)* **605**, 675 (2022).
- [24] P. Magnard *et al.*, Fast and Unconditional All-Microwave Reset of a Superconducting Qubit, *Phys. Rev. Lett.* **121**, 060502 (2018).
- [25] D. Ristè, J. G. van Leeuwen, H.-S. Ku, K. W. Lehnert, and L. DiCarlo, Initialization by Measurement of a Superconducting Quantum Bit Circuit, *Phys. Rev. Lett.* **109**, 050507 (2012).
- [26] C. K. Andersen *et al.*, Entanglement stabilization using ancilla-based parity detection and real-time feedback in superconducting circuits, *npj Quantum Inf.* **5**, 1 (2019).
- [27] J. Ghosh and A. G. Fowler, Leakage-resilient approach to fault-tolerant quantum computing with superconducting elements, *Phys. Rev. A* **91**, 020302(R) (2015).
- [28] M. Suchara, A. W. Cross, and J. M. Gambetta, Leakage suppression in the toric code, *Quantum Inf. Comput.* **15**, 997 (2015).
- [29] M. McEwen *et al.*, Relaxing hardware requirements for surface code circuits using time-dynamics, [arXiv:2302.02192](https://arxiv.org/abs/2302.02192).
- [30] N. C. Brown, M. Newman, and K. R. Brown, Handling leakage with subsystem codes, *New J. Phys.* **21**, 073055 (2019).
- [31] N. C. Brown, A. Cross, and K. R. Brown, Critical faults of leakage errors on the surface code, in *Proceedings of the 2020 IEEE International Conference on Quantum Computing and Engineering (QCE)*(2020), pp. 286–294.
- [32] D. Hayes, D. Stack, B. Bjork, A. C. Potter, C. H. Baldwin, and R. P. Stutz, Eliminating Leakage Errors in Hyperfine Qubits, *Phys. Rev. Lett.* **124**, 170501 (2020).

- [33] F. Battistel, B. Varbanov, and B. Terhal, Hardware-efficient leakage-reduction scheme for quantum error correction with superconducting transmon qubits, *PRX Quantum* **2**, 030314 (2021).
- [34] K. C. Miao *et al.*, Overcoming leakage in scalable quantum error correction, [arXiv:2211.04728](https://arxiv.org/abs/2211.04728).
- [35] M. Grassl, T. Beth, and T. Pellizzari, Codes for the quantum erasure channel, *Phys. Rev. A* **56**, 33 (1997).
- [36] C. H. Bennett, D. P. DiVincenzo, and J. A. Smolin, Capacities of Quantum Erasure Channels, *Phys. Rev. Lett.* **78**, 3217 (1997).
- [37] T. M. Stace, S. D. Barrett, and A. C. Doherty, Thresholds for Topological Codes in the Presence of Loss, *Phys. Rev. Lett.* **102**, 200501 (2009).
- [38] S. D. Barrett and T. M. Stace, Fault Tolerant Quantum Computation with Very High Threshold for Loss Errors, *Phys. Rev. Lett.* **105**, 200502 (2010).
- [39] A. Kubica, A. Haim, Y. Vaknin, F. Brandão, and A. Retzker, Erasure qubits: Overcoming the T_1 limit in superconducting circuits (2022).
- [40] Y. Wu, S. Kolkowitz, S. Puri, and J. D. Thompson, Erasure conversion for fault-tolerant quantum computing in alkaline earth Rydberg atom arrays, *Nat. Commun.* **13**, 4657 (2022).
- [41] J. Heinsoo *et al.*, Rapid High-Fidelity Multiplexed Readout of Superconducting Qubits, *Phys. Rev. Appl.* **10**, 034040 (2018).
- [42] See Supplemental Material at <http://link.aps.org/supplemental/10.1103/PhysRevLett.130.250602> for additional information supporting statements and claims made in the main text, which includes Refs. [2,5–7,24,33,41,43–48].
- [43] J. M. Chow *et al.*, Universal Quantum Gate Set Approaching Fault-Tolerant Thresholds with Superconducting Qubits, *Phys. Rev. Lett.* **109**, 060501 (2012).
- [44] R. Versluis, S. Poletto, N. Khammassi, B. Tarasinski, N. Haider, D. J. Michalak, A. Bruno, K. Bertels, and L. DiCarlo, Scalable Quantum Circuit and Control for a Superconducting Surface Code, *Phys. Rev. Appl.* **8**, 034021 (2017).
- [45] P. Krantz, M. Kjaergaard, F. Yan, T. P. Orlando, S. Gustavsson, and W. D. Oliver, A quantum engineer’s guide to superconducting qubits, *Appl. Phys. Rev.* **6**, 021318 (2019).
- [46] E. Magesan, J. M. Gambetta, and J. Emerson, Characterizing quantum gates via randomized benchmarking, *Phys. Rev. A* **85**, 042311 (2012).
- [47] E. Magesan *et al.*, Efficient Measurement of Quantum Gate Error by Interleaved Randomized Benchmarking, *Phys. Rev. Lett.* **109**, 080505 (2012).
- [48] C. J. Wood and J. M. Gambetta, Quantification and characterization of leakage errors, *Phys. Rev. A* **97**, 032306 (2018).
- [49] http://github.com/DiCarloLab-Delft/Leakage_Reduction_Unit_Data.